# The Effect of PEGylation on Multivalent Binding: A SPR and ITC Study with Structurally Diverse PEG-Dendritic GATG Copolymers

Marcos Fernandez-Villamarin,[a] Ana Sousa-Herves,[a] Juan Correa,[a] Eva Maria Munoz,[a,b] Pablo Taboada,[c] Ricardo Riguera,[a] and Eduardo Fernandez-Megia [a] *

**Abstract:** A general synthetic strategy to PEG-dendritic block copolymers of the GATG family is described from commercially available PEG of different molecular weights and architectures. Glycosylation of the resulting azide-terminated copolymers with fucose by CuAAC afforded a toolbox to study the effect of PEG on the multivalent binding with the lectin UEA-I by SPR (on surface) and ITC (in solution). Our results indicate that PEG reduces the affinity of glycodendrimers towards lectins by steric hindrance in a molecular weight dependent fashion. Great differences were observed as a function of the PEG architecture, with diblock PEG-dendritic copolymers benefiting from a positive entropic contribution (PEG folding), not seen in the dendritic-PEG-dendritic systems. The self-inflicted steric stabilization of the PEGylated copolymers onto lectin clusters reveals the necessity of additional competitive experiments to fully assess the antiadhesive properties of PEG in biological environments.

## Introduction

Multivalent interactions play a key role in nature as efficient recognition tools for controlling a plethora of physiological and pathological events. The presence of multiple copies of ligands and receptors on biological surfaces, which interact with low monovalent affinity, can be exploited in a multivalent fashion for recognition with enhanced selectivity and exponentially increased affinity.[1] Carbohydrate-lectin interactions represent the archetypal illustration of multivalency in nature, mediating major biological processes like cell−cell communication, fertilization or pathogen infection, to mention a few.[2] In this context, the preparation of synthetic multivalent carbohydrates has attracted much attention for triggering or inhibiting natural processes, and as tools to unravel the mechanisms controlling these complex interactions: intermolecular crosslinking, chelation, and statistical rebinding.[3] Among the multivalent scaffolds available, the monodispersity of dendrimers represents a hallmark when interpreting affinity data in terms of size and multivalency.[4]

Our group has recently studied the multivalent interaction between glycosylated GATG (gallic acid−triethylene glycol) dendrimers and the lectin Concavalin A (ConA) by surface plasmon resonance (SPR).[5] These works reveal the importance of performing direct (surface bound lectin), real-time analysis of multivalent interactions in order to disentangle a dynamic binding heterogeneity. Thus, while a population of dendrimers binds the lectin surface monovalently, others display higher functional valences. Moreover, the contribution of the various multivalent mechanisms is a time-dependent feature governed not only by the glycoconjugate multivalency and lectin cluster density, but also by the local concentration of glycoconjugates in the proximity of the lectin cluster.

In addition, seminal reports by Whitesides and coworkers[1b] have proposed an extra “steric stabilization” mechanism to explain the enhanced pathogen-inhibitory activity of large multivalent glycoconjugates. It was suggested that large glycoconjugates upon interaction with pathogens create a water-swollen, gel-like layer that sterically prevents their approximation to host cells. Inspired by this hypothesis, we envisioned the potential anti-adhesive effect of glycosylated PEG-dendritic block copolymers [Figure 1, PEG is poly(ethylene glycol)]. PEG is a linear polymer widely used for biomedical applications, characterized by low toxicity and immunogenicity, and a high aqueous solubility.[6] The incorporation of a single PEG chain at the focal point of dendrimers results in PEG-dendritic block copolymers with increased solubility, stealth properties and long circulation times in the blood stream. Such hybrid linear-dendritic structures have promising applications in drug and gene delivery, tissue repair, and diagnosis.[7]

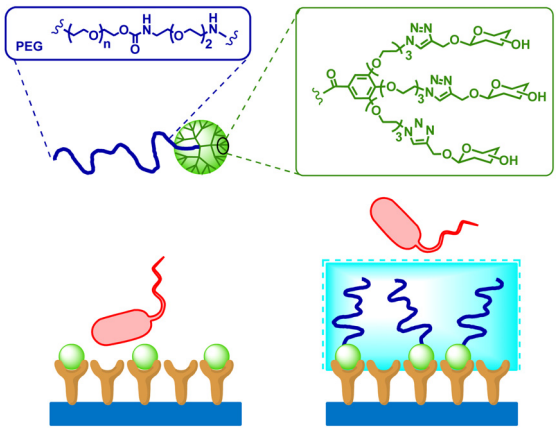


**Figure 1.** Schematic impression of the steric stabilization imparted by glycosylated dendrimers and PEG-dendritic block copolymers bound to lectin clusters.

Our laboratory has recently developed the GATG dendritic family and their block copolymers with PEG as a platform for biomedical applications.[8] GATG dendrimers are composed of a

[a] M. Fernandez-Villamarin, Dr. A. Sousa-Herves, Dr. J. Correa, Dr. E. M. Munoz, Prof. R. Riguera, Prof. E. Fernandez-Megia.
Department of Organic Chemistry and Center for Research in Biological Chemistry and Molecular Materials (CIQUS), University of Santiago de Compostela, Jenaro de la Fuente s/n, 15782 Santiago de Compostela, Spain
E-mail: ef.megia@usc.es
[b] Dr. E. M. Munoz current address. AFFINImeter Scientific and Development team, Software 4 Science Developments, S.L., Ed. Emprendia, Campus Vida, Santiago de Compostela, Spain.
[c] Prof. P. Taboada
Condensed Matter Physics Department, University of Santiago de Compostela, Facultade de Física, Campus Sur, 15782 Santiago de Compostela, Spain

Supporting information for this article is given via a link at the end of the document

repeating unit incorporating a gallic acid core and hydrophilic triethylene glycol arms carrying terminal azides. These can be exploited for the facile decoration of the dendritic periphery with ligands of biomedical interest,[9] including unprotected carbohydrates,[10] by Cu(I)-catalyzed azide-alkyne cycloaddition (CuAAC).[11] Not unexpectedly, besides a superior biocompatibility and solubility, PEG-dendritic copolymers have also resulted in reduced cellular uptake[12] and transfection efficiencies,[13] which have been associated to the stealth effect of PEG. With the ultimate goal of exploring this "steric stabilization" mechanism in antiadhesive therapy, herein we report our efforts oriented to develop a general synthetic strategy to PEG-dendritic block copolymers of the GATG family from commercially available PEG of different molecular weights and architectures. After CuAAC glycosylation, the binding properties of these copolymers have been evaluated towards lectins using two complementary techniques: SPR to analyze the interaction with lectins clustered on a surface, and isothermal titration calorimetry (ITC) with free lectins in solution. With this aim, we have selected α-L-fucose (Fuc), a monosaccharide often found as terminal sugar in glycans that participate in important cell–cell interactions and cell migration events related to physiological and pathological processes, like fertilization, embryogenesis, lymphocyte trafficking, immune responses, and cancer metastasis.[14]

## Results and Discussion

### Synthesis of PEG-GATG block copolymers

Our previous strategy for the preparation of PEG-dendritic block copolymers of the GATG family involved a divergent synthesis starting from a commercially available amino-functionalized PEG of molecular weight 5000 Da (MeO-$PEG_{5000}$-$NH_2$).[10b] Following a "chain first" approach, a copolymer of generation one (G1) was directly obtained by amide coupling between the terminal amine at PEG and the carboxylic acid at the GATG repeating unit. A subsequent azide reduction-amide coupling sequence afforded copolymers up to G4 in high yields.[10b, 15] Noteworthy, this synthetic route takes advantage of the properties of PEG as a soluble polymeric support for the facile purification of all intermediates by precipitation.[16]

In spite of the efficiency of this synthesis, its application for the preparation of block copolymers with PEG of different molecular weights and architectures has been long hampered by the low accessibility, limited structural diversity and uncertain end group purity of commercially available amino-functionalized PEG. To solve this inconvenience, we have decided to prepare PEG-$NH_2$ by incorporating a monoprotected diamino spacer to the more commonly available hydroxy-terminated PEG (PEG-OH). As shown in Scheme 1, by using a carbamate linkage, PEG chains carrying terminal amino groups were readily obtained from linear monohydroxy ($PEG_{2000}$-OH, $PEG_{5000}$-OH), dihydroxy ($PEG_{10000}$-2OH), as well as a 4-arm tetra-hydroxy PEG ($PEG_{20000}$-4OH). To this end, the various PEG-OH were first activated as N-hydroxysuccinimide (NHS) carbonates by reaction with N,N´-disuccinimidyl carbonate (DSC) in a pyridine/$CH_2Cl_2$/$CH_3CN$ mixture. The resulting PEG-NHS were obtained in excellent yields (98-99%) by precipitation. $^1$H NMR spectroscopy of PEG-NHS revealed the presence of a multiplet at ca. 4.4 ppm, corresponding to the methylene protons adjacent to the carbonate group, as well as a singlet at ca. 2.7 ppm corresponding to the succinimide ring protons. Reaction of PEG-NHS with the monoprotected tert-butyl (2-(2-(2-aminoethoxy)ethoxy)ethyl)carbamate[17] ($Et_3N$, $CH_2Cl_2$) led to PEG-NHBoc in excellent yields (96-98%) after purification by precipitation. The disappearance of the peak corresponding to the succinimide protons in the $^1$H NMR spectra of PEG-NHBoc, and the appearance of a new peak around 1.4 ppm corresponding to the tert-butyl group confirmed the completion of the coupling. A final deprotection of the Boc group with TFA in $CH_2Cl_2$ rendered the desired PEG-$NH_2$ in 89-99% yields. NMR spectroscopy confirmed the structure and purity of PEG-$NH_2$. While $^1$H NMR spectra showed complete removal of the Boc group and appearance of a new triplet at ca. 2.9 ppm for the methylene protons adjacent to the amino group, the $^{13}$C NMR revealed a characteristic new peak at ca. 40 ppm corresponding to the methylene carbon in alpha to the amino group. COSY and HMQC spectra further confirmed the structure of all the products in the route. End-group purity of PEG-$NH_2$ and the intermediates was proven by MALDI-TOF MS showing the expected series of 44 Da spaced peaks, and $M_p$, $M_n$ and $M_w$ in agreement with calculated values (Figures 2 and S1). No signals resulting from unreacted starting materials or side products were seen, confirming the purity of the PEG products (full experimental details and characterization in the Electronic Supplementary Information, ESI).

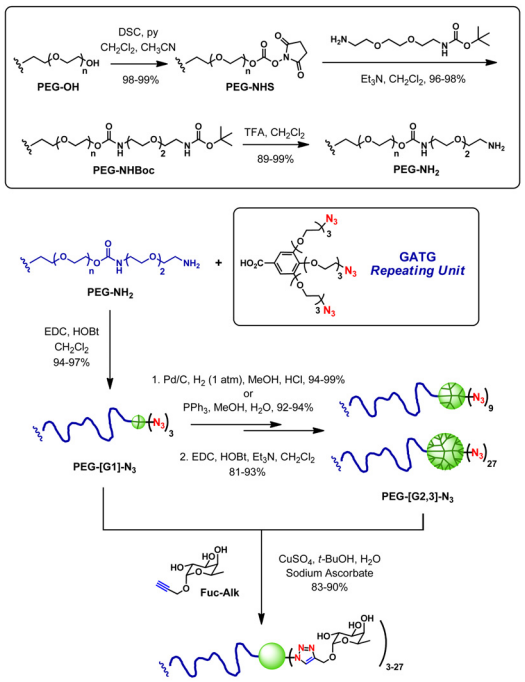


**Scheme 1.** Synthesis of amino-functionalized PEG and PEG-GATG block copolymers, followed by CuAAC peripheral glycosylation.

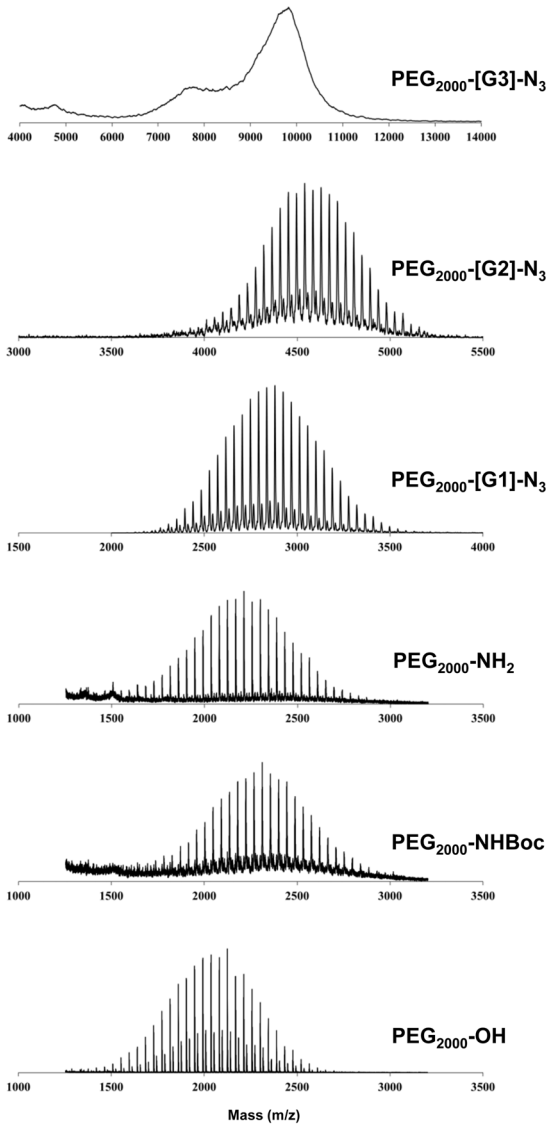


**Figure 2.** MALDI-TOF MS of $PEG_{2000}$ derivatives.

With a reliable and scalable access to a collection of amino-functionalized PEG of different molecular weights and architectures (i.e.; $PEG_{2000}$-$NH_2$, $PEG_{5000}$-$NH_2$, $PEG_{10000}$-$2NH_2$, and $PEG_{20000}$-$4NH_2$), we decided to proceed with the preparation of PEG-GATG copolymers of G1-G3 (Scheme 1 and Figure 3). With this aim, all PEG-$NH_2$ were first covalently linked to the GATG repeating unit via amide bond (EDC, HOBt, $CH_2Cl_2$) to render $PEG_{2000}$-[G1]-$N_3$, $PEG_{5000}$-[G1]-$N_3$, $PEG_{10000}$-2[G1]-$N_3$, and $PEG_{20000}$-4[G1]-$N_3$ in high purity and excellent yields (94-97%), after purification by precipitation (MeOH/iPrOH). These copolymers were completely characterized by NMR, IR and MALDI-TOF (ESI). Characteristic signatures of all G1 copolymers are a triplet around 3.4 ppm by $^1H$ NMR corresponding to the methylene protons adjacent to the azide groups, a peak ca. 50 ppm in the $^{13}C$ NMR spectra corresponding to the methylene carbon alpha to the azides, and an intense IR band around 2100 $cm^{-1}$ typical of the azide group.

MALDI-TOF showed the expected series of 44 Da spaced peaks and molecular weights that confirm the efficiency of the coupling (Figures 2 and S1). Next, block copolymers of G2 and G3 were obtained by sequential reduction of the terminal azides, either by catalytic hydrogenation (Pd/C, 1 atm $H_2$, MeOH, HCl; 94-99% for $PEG_{2000}$, $PEG_{5000}$ and $PEG_{10000}$) or Staudinger reaction ($PPh_3$, MeOH-$H_2O$; ultrafiltration; 92-94% for 4-arm $PEG_{20000}$), followed by incorporation of a new layer of repeating units via amide coupling (EDC, HOBt, $Et_3N$, $CH_2Cl_2$; 81-93%). Again, these steps were easily followed and all products characterized by NMR, IR and MALDI-TOF as seen above (experimental details and characterization in the ESI). This way, block copolymers up to G3, i.e.; $PEG_{2000}$-[G3]-$N_3$, $PEG_{5000}$-[G3]-$N_3$, $PEG_{10000}$-2[G3]-$N_3$, and $PEG_{20000}$-4[G3]-$N_3$, were obtained in excellent yields in a routine basis (Figure 3).

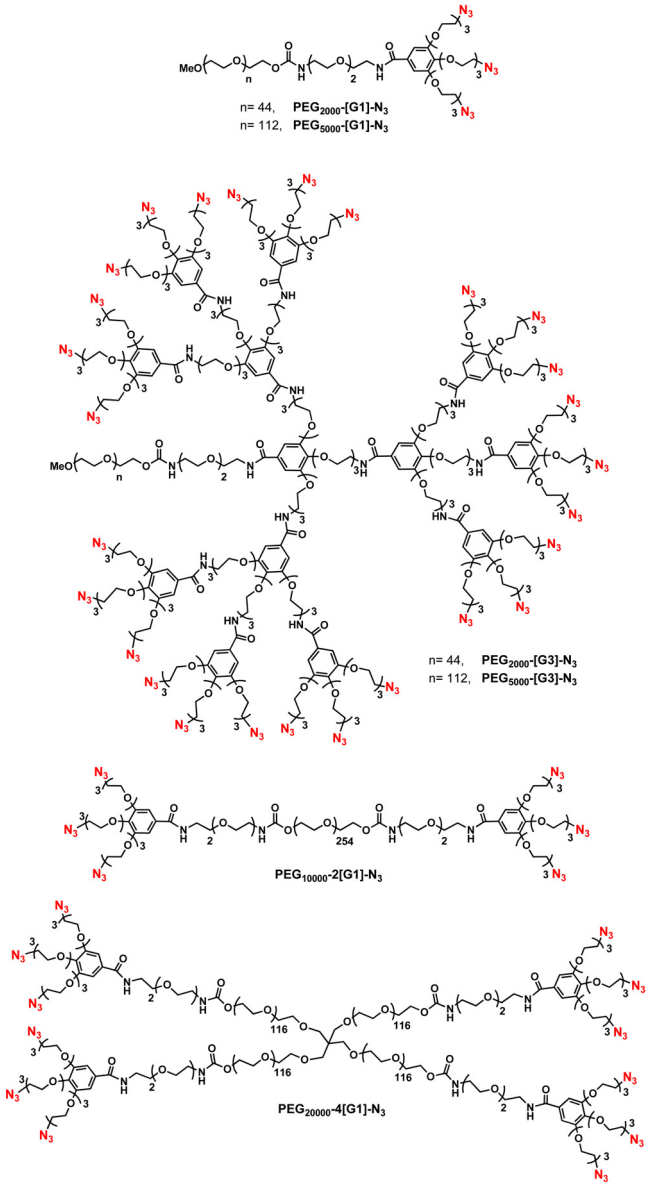


**Figure 3.** Structure of representative PEG-GATG block copolymers.

**CuAAC glycosylation of PEG-GATG block copolymers**

The multivalent peripheral decoration of the PEG-GATG block copolymers with unprotected carbohydrates was straightforward by CuAAC as described by our group.[10b] The monosaccharide α-L-Fuc was selected based of its relevance in multivalent cell-cell interactions and cell migration processes.[14] The coupling of an alkynated Fuc derivative (Fuc-Alk) to PEG-GATG was performed in the presence of catalytic amounts of $CuSO_4$ (1 mol% per terminal azide) and sodium ascorbate (5 mol% per terminal azide) in t-BuOH/$H_2O$. The resulting fucosylated derivatives were readily obtained in very good yields (83-90%) after purification by ultrafiltration (Scheme 1). Complete functionalization of the dendritic periphery was confirmed by $^1$H NMR ($D_2O$) thanks to the disappearance of the signal corresponding to the methylene protons adjacent to the azide groups, and by the loss of the characteristic azide band at ca. 2100 $cm^{-1}$ in IR (Figure S2). At the same time, new signals in $^1$H NMR around 4.9-5.0 (anomeric) and 8.0-8.1 ppm (triazol protons) confirmed the incorporation of Fuc.

With this library of fucosylated PEG-dendritic block copolymers in hand (Table S1), we proceeded to study their binding behavior with the lectin ulex europaeus agglutinin I (UEA-I), a homodimeric lectin (each subunit is approximately 27 kDa) from gorse seeds that shows high affinity and specificity for α-L-Fuc.[18] Two complementary techniques were used: SPR with lectins clustered on a chip surface, and ITC with the free lectin in solution. To elucidate the effect of PEG, experiments were also performed with previously synthesized non-PEGylated dendrimers[10a] for comparison purposes.

**SPR experiments**

To perform SPR direct experiments, UEA-I was covalently bound to a polycarboxylate sensor chip ($RU_{immo}$ = 10300 μRiU; 1 μRiU ~ 1 pg/$mm^2$) via standard amino coupling. As control experiment, the binding of the monosaccharide Fuc-Alk was first evaluated by sequentially injecting increasing concentrations of the analyte over the lectin surface. As expected for a monovalent saccharide-lectin interaction, fast association and dissociation steps were observed (Figure 4). Based on previous reports by our group,[5b] a steady state analysis of the sensorgrams was performed, and the binding isotherm was fitted to a 1:1 Langmuir model (Figure S3) to yield a dissociation constant ($K_D^{SPR}$) of 103 μM (Table 1). This experiment also proved that around 70% of the lectin remained active after immobilization on the chip surface. Then, the SPR analysis was performed with fucosylated PEG-GATG copolymers of various generations, multivalency and architecture, i.e.; $PEG_{2000}$-[G2]-Fuc, $PEG_{5000}$-[G2,3]-Fuc, $PEG_{10000}$-2[G2,3]-Fuc and $PEG_{20000}$-4[G2]-Fuc. The non-PEGylated systems [G2]-Fuc and [G3]-Fuc[10a] were also included in the analysis.

The sensorgrams of the interaction of the PEGylated glycodendrimers with the lectin surface showed a much more complex binding profile than Fuc-Alk, in agreement with the multivalent-heterogeneous nature of these complex interactions (Figure 4). Fast-on rate bindings were followed by slower two-step dissociation processes. Unfortunately, binding constants for $PEG_{20000}$-4[G2]-Fuc could not be obtained because of partial aggregation of this high molecular weight sample. A steady state analysis of each SPR experiment was performed to obtain binding information in the equilibrium state, which is more suitable for direct comparison with data obtained by ITC measurements in solution. In all cases the corresponding isotherm was fitted to a two-site binding model, indicative of a fraction of the dendrimers binding the lectin surface with higher affinity and the remaining dendrimers with lower affinity (Figure S3).[5b] This analysis provided a $K_D^{SPR}$ and a maximum SPR response ($R_{max}$) for each binding type. $R_{max}$ values were normalized to account for the number of glycoconjugate species binding to the lectin surface. With these data, a weighted average $K_D^{SPR}$ was calculated as an estimation of the overall binding efficiency of each dendritic system towards the lectin surface (Table 1).

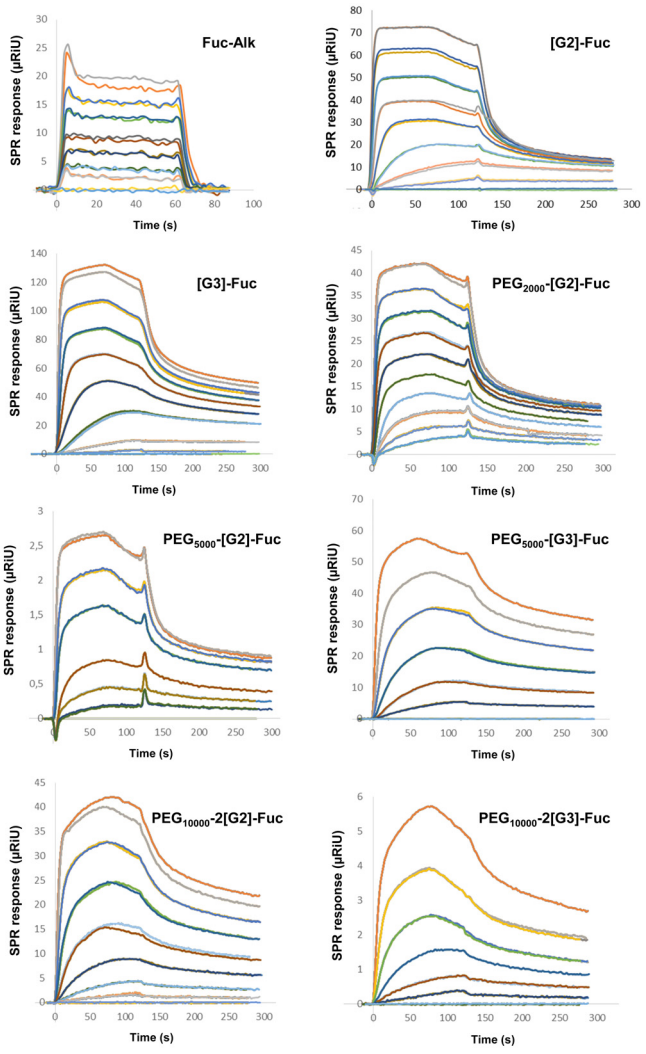


**Figure 4.** Sensorgrams of Fuc-Alk (643-10.0 μM), [G2]-Fuc (75.2-0.03 μM), [G3]-Fuc (25-0.01 μM), $PEG_{2000}$-[G2]-Fuc (75.2-0.15 μM), $PEG_{5000}$-[G2]-Fuc (75.2-0.19 μM), $PEG_{5000}$-[G3]-Fuc (25-0.10 μM), $PEG_{10000}$-2[G2]-Fuc (75.2-0.10 μM) and $PEG_{10000}$-2[G3]-Fuc (12.5-0.05 μM) binding to UEA-I.

**Table 1.** Binding parameters obtained from the steady state analysis of SPR experiments with UEA-I

| Dendrimer | Average | | High affinity | | Low affinity | | F[b] |
|---|---|---|---|---|---|---|---|
| | $K_D^{SPR}$ (μM) | $R_{max}$[a] | $K_{D\text{-}high}^{SPR}$ (μM) | $R_{max\text{-}high}$[a] | $K_{D\text{-}low}^{SPR}$ (μM) | $R_{max\text{-}low}$[a] | |
| **Fuc-Alk** | 103 | 212 | - | - | - | - | - |
| **[G2]-Fuc** | 2.73 | 87 | 0.28 | 40 | 19 | 47 | 0.46 |
| **[G3]-Fuc** | 2.26 | 60 | 0.22 | 29 | 20 | 31 | 0.48 |
| **$PEG_{2000}$-[G2]-Fuc** | 6.94 | 55 | 0.89 | 24 | 34 | 31 | 0.44 |
| **$PEG_{5000}$-[G2]-Fuc** | 7.34 | 31 | 1.45 | 14 | 31 | 17 | 0.45 |
| **$PEG_{5000}$-[G3]-Fuc** | 2.95 | 25 | 0.87 | 14 | 14 | 11 | 0.56 |
| **$PEG_{10000}$-2[G2]-Fuc** | 8.77 | 16 | 1.66 | 7 | 32 | 9 | 0.44 |
| **$PEG_{10000}$-2[G3]-Fuc** | 5.02 | 10 | 0.39 | 3 | 15 | 7 | 0.30 |

[a] $R_{max}$ obtained after analysis of normalized sensorgrams where the SPR response was divided by the molecular weight of the analyte and multiplied by 1000. [b] Estimated fraction of dendrimer binding with a high affinity binding mode; calculated as $R_{max\text{-}high}/(R_{max\text{-}high} + R_{max\text{-}low})$.

All the glycodendrimers present averaged $K_D^{SPR}$ values in the low micromolar range, indicative of a binding efficiency between 12 and 46 times higher than the corresponding monosaccharide (Table 1). Notably, the analysis revealed no significant differences in the binding properties of [G2]-Fuc and [G3]-Fuc towards the lectin surface. This finding differs from our previous observations with mannosylated dendrimers and the tetrameric lectin Concanavalin A,[5b] which can be attributed to structural differences of the lectins and lectin density within the sensor chip. Nevertheless, the normalized $R_{max}$ calculated for [G2]-Fuc was markedly higher than the value obtained for [G3]-Fuc. This demonstrates that the lectin surface can accommodate a higher number of [G2]-Fuc, due to its smaller size compared with [G3]-Fuc. In order to understand the effect of incorporating PEG chains of different length to the dendritic block, $PEG_{2000}$-[G2]-Fuc and $PEG_{5000}$-[G2]-Fuc were analyzed. Table 1 shows that the global binding efficiency of $PEG_{2000}$-[G2]-Fuc and $PEG_{5000}$-[G2]-Fuc decreased by 2.5 and 2.7 fold, respectively, as compared to [G2]-Fuc. This is the result of a decrease in the binding efficacy of both high and low affinity binding modes, being the effect more pronounced in the high affinity mode. Thus, $K_{D\text{-}high}^{SPR}$ of $PEG_{2000}$-[G2]-Fuc and $PEG_{5000}$-[G2]-Fuc is 3.2 and 5.2 times higher than the $K_{D\text{-}high}^{SPR}$ of [G2]-Fuc. Moreover, the $R_{max}$ decreased notably, especially in the case of $PEG_{5000}$-[G2]-Fuc. The same trend was observed when $PEG_{5000}$ was incorporated into [G3]-Fuc, with a 4.0-fold increase in $K_{D\text{-}high}^{SPR}$. This fact is pointing out that the presence of the PEG results in a high steric hindrance, which ultimately lowers the number of glycodendrimers that can simultaneously bind to the lectin cluster. Additionally, it lowers the intrinsic binding efficiency of the dendrimer and weakens the multivalent effect. The penalty paid by the presence of PEG seems to be less pronounced at higher dendrimer/PEG molecular weight ratios. In that sense, $PEG_{2000}$-[G2]-Fuc shows a higher affinity than $PEG_{5000}$-[G2]-Fuc, while $PEG_{5000}$-[G3]-Fuc binds to the lectin cluster in a higher extension than $PEG_{5000}$-[G2]-Fuc.

The steady state analysis of the interaction of the copolymers displaying two GATG dendritic blocks per PEG chain, $PEG_{10000}$-2[G2]-Fuc and $PEG_{10000}$-2[G3]-Fuc, yielded $K_D^{SPR}$ values higher than those obtained for the corresponding non-PEGylated dendrimers, but surprisingly are in the range of $PEG_{5000}$-[G2]-Fuc and $PEG_{5000}$-[G3]-Fuc. In addition, they present the lowest $R_{max}$ among the glycodendrimers tested. This result suggests that the incorporation of a second dendritic block to the structure does not increase the binding efficiency when the lectin is clustered on a surface. That is, only one dendritic block participates in the binding to the lectin surface. In addition, it corroborates that an increase in the size of the PEG chain results in a stronger steric hindrance and weaker binding efficiency. Again, these effects are less pronounced in the fucosylated copolymer of G3 than the G2 counterpart.

From SPR it can be concluded that PEG decreases the affinity of glycodendrimers towards target lectins on a surface. Also, that the steric effect of PEG plays a key role in reducing the number of glycodendrimers nearby the lectin surface ($R_{max}$), which for antiadhesive purposes would eventually result in a lower density of PEGylated glycodendrimers on the pathogen/cell surface and so, a thinner gel-like layer than pursued for preventing infection.

**Table 2.** Binding parameters obtained from ITC experiments with UEA-I

| Dendrimer | Struct. valency | rM | Funct. valency[a] | RatioFunct Fuc[b] | $K_A^{ITC}(M^{-1})$ | $K_D^{ITC}$ (μM) | $\Delta H^{ITC}$ (cal/mol) | $T^*\Delta S^{ITC}$ (cal/mol) | $\Delta G^{ITC}$ (cal/mol) |
|---|---|---|---|---|---|---|---|---|---|
| **Fuc** | 1 | - | - | - | 6410 | 156.00 | -6000 | -809 | -5191 |
| **$PEG_{5000}$-[G1]-Fuc** | 3 | 0.45764 | 2.2 | 72.8 | 196490 | 5.09 | -3793 | 3425 | -7218 |
| **$PEG_{5000}$-[G2]-Fuc** | 9 | 0.23165 | 4.3 | 48.0 | 414900 | 2.41 | -3579 | 4081 | -7660 |
| **$PEG_{5000}$-[G3]-Fuc** | 27 | 0.17591 | 5.7 | 21.1 | 2432700 | 0.41 | -2592 | 6116 | -8708 |
| **$PEG_{10000}$-2[G1]-Fuc** | 6 | 0.31628 | 3.2 | 52.7 | 129240 | 7.74 | -13764 | -6794 | -6970 |
| **$PEG_{10000}$-2[G3]-Fuc** | 54 | 0.11990 | 8.3 | 15.4 | 276060 | 3.62 | -32826 | -25407 | -7419 |

[a] Functional valency represents the number of Fuc residues participating in the binding to the lectin. It is calculated as the inverse of the parameter rM that accounts for the stoichiometry of binding (see more details in the ESI). [b] Ratio of functional Fuc calculated as (Functional valency/Structural valency)*100.

### ITC experiments

With the aim of better understanding the interaction of the PEGylated copolymers with the lectin cluster, ITC measurements were performed with UEA-I in solution. ITC measures heats of association for receptor-ligand interactions as one of the components is titrated into the other. When these heats are analyzed as a function of the concentration of the ligand relative to the receptor, values for the enthalpy of binding ($\Delta H^{ITC}$) and binding constants ($K_A^{ITC} = 1/K_D^{ITC}$) are determined. The binding parameters for $PEG_{5000}$-[Gn]-Fuc and $PEG_{10000}$-2[Gn]-Fuc obtained from ITC experiments with UEA-I are depicted in Table 2 (Figures S4-S8).

$PEG_{5000}$-[G1]-Fuc and $PEG_{5000}$-[G2]-Fuc show $K_D^{ITC}$ values in the low micromolar range, indicative of a binding efficiency between 31 and 65 times higher than the corresponding monosaccharide.[19] When $PEG_{5000}$-[G3]-Fuc was analyzed, an even larger binding efficiency (380-fold higher than the monosaccharide) was observed. As expected, the functional valency in this series (which represents the number of effective Fuc residues participating in the binding) increases with G (Table 2). When moving to the $PEG_{10000}$-2[Gn]-Fuc series, low micromolar affinities were also shown. Interestingly, the functional valency in this system increased compared to the same G in $PEG_{5000}$-[Gn]-Fuc, indicating that in solution both dendritic blocks of $PEG_{10000}$-2[Gn]-Fuc participate in the binding with the lectin as opposed to surface bound experiments. Despite this, the binding of a lower ratio of functional Fuc in $PEG_{10000}$-2[Gn]-Fuc (defined as the proportion between functional and structural valencies) results in slightly larger values of $K_D$ compared to $PEG_{5000}$-[Gn]-Fuc.[20]

Lastly, Table 3 compiles the values obtained for the thermodynamic parameters $\Delta H^{ITC}$ and $\Delta S^{ITC}$ normalized to the functional valency of each copolymer. The information extracted from the entropic and enthalpic contributions to binding follows a trend analogous to that found in other multivalent lectin–glycoconjugate interactions.[21] In addition, some differences in the thermodynamic paramaters are observed between $PEG_{5000}$-[Gn]-Fuc and $PEG_{10000}$-2[Gn]-Fuc. The favourable enthalpic contribution for the $PEG_{10000}$-2[Gn]-Fuc series arises from the formation of direct and water-mediated hydrogen bonds, dipolar and London dispersive forces, while the negative entropic term might be attributed to the loss of degrees of freedom of the ligand upon binding, as seen in the monosaccharide.[22] This behavior is rather different for $PEG_{5000}$-[Gn]-Fuc, in which negative enthalpic terms are accompanied by an increase in $\Delta S^{ITC}$. This difference may originate from the contribution of a strong adsorption of the PEG onto the surface of the dendrimer–lectin complex, resembling in some manner the formation of an aggregated species, where the release of structurally ordered water molecules from the hydration shells of PEG chains brought close to the complex might account for the significantly favourable entropic contribution observed.

Indeed, the folding of PEG onto dendritic systems has been througly studied by molecular simulations[23] and more recently using well-tempered metadynamics (WT-MetaD) simulation.[24] Pavan and coworkers have described that PEG chains, despite their linear character, tend to fold in solution assuming a stable compact globular shape that can collapse and compactly wrap dendrimers. These authors proposed that PEG folding limits water penetration inside the dendritic scaffold, thereby increasing their molecular hydrophobicity, which could be at the origin of the aggregation observed in some PEGylated dendrimers.[24-25]

**Table 3.** ITC thermodynamic parameters relative to the functional valency

| Dendrimer | $\Delta H^{ITC}$ (cal/mol) | $T^*\Delta S^{ITC}$ (cal/mol) | $\Delta G^{ITC}$ (cal/mol) |
|---|---|---|---|
| **Fuc** | -6000 | -809 | -5191 |
| **$PEG_{5000}$-[G1]-Fuc** | -1736 | 1567 | -3303 |
| **$PEG_{5000}$-[G2]-Fuc** | -829 | 945 | -1775 |
| **$PEG_{5000}$-[G3]-Fuc** | -456 | 1076 | -1532 |
| **$PEG_{10000}$-2[G1]-Fuc** | -4353 | -2149 | -2204 |
| **$PEG_{10000}$-2[G3]-Fuc** | -3936 | -3046 | -890 |

On the contrary, the impact on molecular hydrophilicity and PEG adsorption would be precluded for $PEG_{10000}$-2[Gn]-Fuc since the two dendritic blocks at the distal ends of the PEG chain restrict the degrees of freedom in this case. This observation also agrees with previous molecular dynamics findings by Hawker and coworkers on an alternative PEG-2[G4] system, where the PEG was proposed to collapse into a central globular shape with the dendrons exposed at both sides.[26] In our case, this situation would lead to an increased interaction of the dendrons with the surrounding aqueous environment, and in the absence of a sizable PEG wrapping, to a negative entropic contribution.

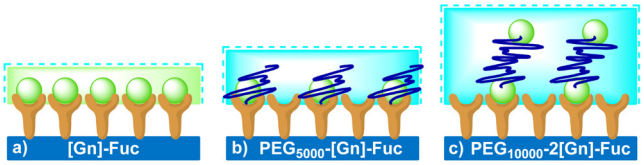


**Figure 5.** The steric hindrance of PEG reduces the affinity of glycodendrimers towards lectins and lowers their density coverage ($R_{max}$ in SPR) on lectin clusters in the order [Gn]-Fuc < $PEG_{2000}$-[Gn]-Fuc < $PEG_{5000}$-[Gn]-Fuc < $PEG_{10000}$-2[Gn]-Fuc. While the interaction of PEG-[Gn]-Fuc (b) with lectin UEA-I is characterized by a positive $\Delta S^{ITC}$ contribution associated to the folding of the PEG onto the dendrimer–lectin complex, the restricted freedom and more exposed dendritic blocks in PEG-2[Gn]-Fuc (c) hamper this stabilizing PEG wrapping (negative $\Delta S^{ITC}$), ultimately affording a reduced affinity and just one fully functional dendritic block in surface bound experiments.

## Conclusions

With the ultimate goal of exploring the "steric stabilization" of linear-dendritic copolymers in antiadhesive therapy, we describe a general synthetic procedure to PEG-dendritic block copolymers of the GATG (gallic acid−triethylene glycol) family from commercially available hydroxy-terminated PEG of different molecular weights and architectures, i.e.; monohydroxy ($PEG_{2000}$-OH, $PEG_{5000}$-OH), dihydroxy ($PEG_{10000}$-2OH), and 4-arm tetra-hydroxy ($PEG_{20000}$-4OH) PEG chains. Remarkably, this route circumvents the lower commercial accessibility, limited structural diversity and uncertain end group purity of amino-functionalized PEG. After incorporating a tri(ethylene glycol) diamino linker and following an amide couplig–azide reduction sequence, three generations of PEG-GATG copolymers carrying terminal azides were readily obtained in excellent yields in a routine basis (Scheme 1 and Figure 3). Subsequent complete glycosylation with fucose via CuAAC afforded a structurally diverse collection of copolymers as tools to study the effect of the molecular weight and architecture of PEG on the multivalent binding with lectins. To this end, the lectin ulex europaeus agglutinin I (UEA-I), a homodimeric lectin with high affinity and specificity for α-L-Fuc, was selected. Two complementary techniques were used: surface plasmon resonance (SPR) to analyze the interaction with UEA-I clustered on a surface, and isothermal titration calorimetry (ITC) with the free lectin in solution.

Our results indicate that PEG reduces the affinity of glycodendrimers towards target lectins by steric hindrance, an effect that increases with the molecular weight of the PEG chain (Tables 1-3). In addition, great differences were observed depending on the PEG architecture: PEG-[Gn]-Fuc vs PEG-2[Gn]-Fuc. $PEG_{5000}$-[Gn]-Fuc is characterized by a positive entropic contribution in the binding with UEA-I in solution (ITC), which has been associated to the folding of the PEG onto the dendrimer–lectin complex and the concomitant release of structurally ordered water molecules. Figure 5b shows a schematic representation of this PEG folding for $PEG_{5000}$-[Gn]-Fuc bound to a UEA-I cluster. The restricted freedom and higher exposure of the dendritic blocks in $PEG_{10000}$-2[Gn]-Fuc limits the extent of this stabilizing PEG wrapping (ITC), ultimately affording a system of lower affinity where only one of the dendritic blocks remains functional in surface bound experiments, as shown by SPR and depicted in Figure 5c.

The steric hindrance of PEG also results in lower density coverages onto lectin clusters in surface bound experiments. The $R_{max}$ in SPR drops on going from [Gn]-Fuc to $PEG_{2000}$-[Gn]-Fuc, $PEG_{5000}$-[Gn]-Fuc and $PEG_{10000}$-2[Gn]-Fuc (Table 1 and Figure S3). This effect can be ascribed to PEGylated glycodendrimers already bound to the lectin surface actively preventing further binding of dendrimers by a self-inflicted steric stabilization mechanism (Figure 5). Since the experimental setups described here cannot unveil the relative weight between this increased steric stabilization and the reduced affinity imposed by PEG, additional biological competitive experiments will be required to fully assess the antiadhesive properties of PEG-GATG copolymers towards pathogens as a function of the PEG size, loading and architecture. Finally, because affinity and steric stabilization in PEG-dendritic copolymers depend on the relative size and G of PEG and the dendritic block, this ratio comes up as a key parameter that needs to be optimized when designing these multivalent macromolecules for antiadhesive purposes and other bioapplications.

## Experimental Section

### Materials and methods

MeO-$PEG_{2000}$-OH ($M_n$ 2019, $M_w$ 2041 by MALDI-TOF), MeO-$PEG_{5000}$-OH ($M_n$ 5056, $M_w$ 5088 by MALDI-TOF) and $PEG_{10000}$-2OH ($M_n$ 11199, $M_w$ 11235 by MALDI-TOF) were purchased from Fluka. $PEG_{20000}$-4OH ($M_n$ 20594, $M_w$ 20616 by MALDI-TOF) was obtained from Nektar. 3,4,5-Tri-[2-[2-(2-azidoethoxy)ethoxy]ethoxy]benzoic acid (GATG repeating unit),[27] tert-butyl (2-(2-(2-aminoethoxy)ethoxy)ethyl)carbamate[17] and 2-propynyl α-L-fucopyranoside (Fuc-Alk)[10a] were prepared following previously reported procedures. UEA-I was purchased from Vector laboratories. SPR HC1000 sensor chip was purchased from Xantec bioanalytics. All other chemical and reagents were purchased from commercial sources and used as received unless otherwise stated. All solvents were HPLC grade. $CH_2Cl_2$, $Et_3N$, py, and $CH_3CN$ were distilled from $CaH_2$. Milli-Q water was obtained using a Millipore water purification system. Ultrafiltration was performed on stirred cells with Amicon YM1, Amicon YM3 or Spectrum Molecular/Por (MWCO 1000) membranes.

NMR spectra were recorded on 300, 400 and 500 MHz spectrometers in $D_2O$ or $CDCl_3$. Chemical shifts are reported in ppm (δ units) downfield from tetramethylsilane ($CDCl_3$) or the HOD signal ($D_2O$). All spectra were analyzed with MestReNova software. IR analysis were performed using a Bruker IFS-66v or a Perkin-Elmer Spectrum Two spectrophotometers. MALDI-TOF MS experiments were carried out on a Bruker Autoflex or an Applied Biosystems/MDS SCIEX 4800 MALDI-TOF/TOF spectrometers, using 2-(4-hydroxyphenylazo)benzoic acid (HABA) or 2,5-dihydroxybenzoic acid (DHB) as matrixes and operating in linear mode for the compounds of higher molecular weights.

### Synthesis and glycosylation of PEG-GATG block copolymers

In the following paragraphs, general procedures for the synthesis of PEG-GATG block copolymers and their glycosylation by CuAAC are included. Detailed synthetic conditions and characterization of all compounds is included in the ESI.

General procedure (I) for the preparation of PEG-NHS.
Commercially available PEG-OH were dissolved in a mixture of dry pyridine, $CH_2Cl_2$ and $CH_3CN$ (1:8:2, 0.09 M of hydroxyl groups) under Ar. Then, DSC (2.5 eq per hydroxyl group) was added and the resulting solutions were stirred at rt overnight. Afterwards, reaction mixtures were concentrated, precipitated from $CH_2Cl_2/Et_2O$ and filtrated to give PEG-NHS as white solids.

General procedure (II) for the preparation of PEG-NHBoc.
tert-Butyl (2-(2-(2-aminoethoxy)ethoxy)ethyl)carbamate (5 eq per NHS carbonate group) and $Et_3N$ (3 eq per carbonate group) were dissolved in dry $CH_2Cl_2$ under Ar. Then, PEG-NHS were added (0.05 M of NHS carbonate groups) and the resulting mixtures were stirred at rt overnight. After solvent evaporation, crude products were purified by precipitation from $CH_2Cl_2/Et_2O$.

General procedure (III) for the preparation of PEG-$NH_2$.
TFA (0.25-0.5 mL per 100 mg of PEG-NHBoc) was added to solutions of PEG-NHBoc in $CH_2Cl_2$ (0.01 M of NHBoc groups). After 2 h of stirring at rt, the solvent was evaporated and the crude products were dissolved in sat. $NaHCO_3$. The resulting solutions were extracted with $CHCl_3$ (3x) and the combined organic phases were washed with brine, dried ($Na_2SO_4$) and concentrated to yield PEG-$NH_2$.

General procedure (IV) for the preparation of PEG-[G1]-$N_3$.
PEG-$NH_2$ and the GATG repeating unit (2 eq per amino group) were dissolved in dry $CH_2Cl_2$ under Ar (0.1-0.25 M of amino groups). Then, HOBt (3 eq per amino group) and EDC·HCl (3 eq per amino group) were added. After 24 h of stirring at rt, the reaction mixtures were concentrated and precipitated from MeOH/iPrOH to give PEG-[G1]-$N_3$ as white powders.

General procedure (V) for the azide reduction of PEG-[G1,2]-$N_3$.
Pd/C (20 wt%) and 3 M HCl (1.5 eq. per azide group) were added to degassed solutions of PEG-[G1,2]-$N_3$ in MeOH (0.1 M of azide groups). The resulting mixtures were stirred under $H_2$ (1 atm) overnight. Then, the catalyst was removed by filtration through Celite® and the filtrates were concentrated to give PEG-[G1,2]-$NH_2$·HCl. Reduction of azides in $PEG_{20000}$-4[G1,2]-$N_3$ was done via Staudinger reaction as follows (General procedure VI). $PPh_3$ (1.2 eq per azide group) was added to solutions of $PEG_{20000}$-4[G1,2]-$N_3$ in MeOH:$H_2O$ (98:2) (2 mM of azide groups) and the resulting mixtures were stirred at rt overnight. After addition of 3 M HCl (2 eq per amino group), the solvent was evaporated, and the crude products were purified by ultrafiltration [MeOH:$H_2O$ (1:1), 5 x 30 mL] and lyophilized to afford $PEG_{20000}$-4[G1,2]-$NH_2$·HCl.

General procedure (VII) for the preparation of PEG-[G2,3]-$N_3$.
PEG-[G1,2]-$NH_2$·HCl, GATG repeating unit (2 eq per amino group) and $Et_3N$ (2 eq per amino group) were dissolved in dry $CH_2Cl_2$ under Ar (0.25-0.1 M of amino groups). Then, HOBt (2 eq per amino group) and EDC·HCl (2 eq per amino group) were added. After 12-24 h of stirring at rt, the reaction mixtures were concentrated under vacuum and purified by precipitation (MeOH/iPrOH) or ultrafiltration [MeOH:$H_2O$ (1:1), 5 x 30 mL] to afford, after filtration or lyophilization, PEG-[G2,3]-$N_3$ as white or pale yellow powders.

General procedure (VIII) for the multivalent glycosylation of PEG-GATG block copolymers.
Fuc-Alk (2 eq per azide group) and solutions of $CuSO_4$ (0.01 eq per azide) and sodium ascorbate (0.05 eq per azide) were added to solutions of PEG-[G1,2,3]-$N_3$ in t-BuOH:$H_2O$ (1:1) (0.1 M of azide groups). The resulting solutions were stirred at rt for 24-72 h, and then were purified by ultrafiltration [acetone:$H_2O$ (1:1), 5 x 30 mL) and lyophilized to give pure PEG-[G1,2,3]-Fuc.

**SPR Binding Assays**

Running buffer for SPR experiments consisted of 10 mM HEPES, pH 7.4, 150 mM NaCl, 0.05% Tween 20. All binding studies were performed at 25 °C using a SR7000DC Reichert spectrometer optical biosensor.

Preparation of UEA-I–coated sensor surface.
UEA-I was immobilized at a density of 10300 μRiU to a polycarboxylated hydrogel coated gold surface (HC1000 sensor chip) via amino-coupling procedure,[28] using HEPES as running buffer and a flow rate of 10 μL/min. The surface was activated with 0.05 M NHS/0.2 M EDC·HCl (10 min), and functionalized by injecting a solution of UEA-I (0.7 mg/mL, 10 min) in sodium acetate buffer pH 4.0. Finally, unreacted NHS esters were deactivated with 1 M ethanolamine, pH 8.5 (10 min). Analogously, a control flow cell was treated with NHS/EDC·HCl followed by ethanolamine.

SPR Direct Binding Assays.
A concentration series of Fuc-Alk (643, 321.5, 160.8, 80.4, 40.2, 20.1 and 10.0 μM), [G2]-Fuc (75.2, 25.1, 8.4, 2.8, 0.93, 0.31, 0.10 and 0.03 μM), [G3]-Fuc (25, 8.3, 2.8, 0.93, 0.31, 0.10, 0.03 and 0.01 μM), $PEG_{2000}$-[G2]-Fuc (75.2, 37.6, 18.8, 9.4, 4.7, 2.4, 1.2, 0.59, 0.29 and 0.15 μM), $PEG_{5000}$-[G2]-Fuc (75.2, 25.1, 8.4, 1.7, 0.56 and 0.19 μM), $PEG_{5000}$-[G3]-Fuc (25, 8.3, 2.8, 0.93, 0.31 and 0.10 μM), $PEG_{10000}$-2[G2]-Fuc (75.2, 25.1, 8.4, 2.8, 0.94, 0.31 and 0.10 μM) and $PEG_{10000}$-2[G3]-Fuc (12.5, 4.2, 1.4, 0.46, 0.15 and 0.05 μM) were injected in duplicate for binding to UEA-I (60 s for Fuc-Alk and 120 s in the case of the glycodendrimers). The binding responses were concentration-dependent and the duplicate analyses of each analyte concentration overlaid, indicating that the assay was reproducible. Between binding cycles, the UEA-I–coated surface was regenerated with 70 mM fucose (60 s) in running buffer. Experimental data were corrected for instrumental and bulk artefacts by double referencing to a control sensor chip surface and buffer injections using Scrubber2 software (BioLogic Software v2.0b).

**ITC measurements**

The energetics of the interactions between the different glycodendrimers and UEA-I was evaluated by ITC (VP-ITC MicroCal Inc., Northampton, MA). The experiments were carried out at least in triplicate (variability < 5%) in $H_2O$ at 25 ºC, titrating the dendrimer solution (0.29 mM) onto the protein solution (0.015 mM). A degassed aliquot (1.436 mL) of the stock UEA-I solution was filled in the reaction cell, an identical volume of medium without protein was placed in the reference cell, and 300 μL of different degassed dendrimer solution were loaded in the titration syringe. The binding experiment involved 37 sequential additions of small aliquots (8 μL) of the glycodendrimer solution in the reaction cell under continuous stirring (286 rpm). After each addition, the heat effect was recorded. Control experiments were carried out under identical conditions to obtain the heats of dilution of dendrimer solutions into $H_2O$. The injection schedule (number of injections, volume of injection, and time between injections) was set up using interactive software, all data being stored in a computer. In order to estimate the net reaction enthalpy, the dilution enthalpies were subtracted from the apparent titration heats.

The direct analysis of ITC data curves for glycodendrimer binding to UEA-I allowed the determination of the binding enthalpy ($\Delta H_i^{ITC}$) and entropy change ($\Delta S_i^{ITC}$) of dendrimer binding, and the apparent binding constants ($K_i^{ITC}$) with the number of binding sites ($n_i$), in the *i*-th class of binding site, as follows:

$$Q(i) = M_t V_0 \sum_{i=1}^{m} n_i \theta_i \Delta H_i^{ITC} \qquad (1)$$

where $Q(i)$ is the heat evolved after *i*-th injection, $M_t$ the total concentration of the protein, $V_0$ the active cell volume, and $\theta_i$ the fraction of sites occupied by the glycodendrimer. However, the parameter of

interest for comparison with experiment is the change in heat content from the completion of the *i*-1 injection to completion of the *i* injection. Therefore, after completing an injection, it is necessary to make a correction for displaced volume. The correct expression then for heat released, $\Delta Q(i)$, from the *i*-th injection is:

$$\Delta Q(i) = Q(i) + \frac{dV_i}{V_0}\left[\frac{Q(i)+Q(i-1)}{2}\right] - Q(i-1) \quad (2)$$

The data were analyzed considering two binding sites by the software Affinimiter. After subtraction of the heat of dilution, a non-linear least-squares algorithm and the concentrations of the titrant and sample were used to fit (minimization of $\chi^2$) the heat flow per aliquot, providing best fit values of the stoichiometry ($n_i$), changes in enthalpy ($\Delta H_i^{ITC}$), in entropy ($\Delta S_i^{ITC}$) and binding constants ($K_i^{ITC}$). Gibbs free energy ($\Delta G_i^{ITC}$) was calculated using the expression:

$$\Delta G_i^{ITC} = -RT\ln K_i^{ITC} = \Delta H_i^{ITC} - T\Delta S_i^{ITC} \quad \textbf{(3)}$$

in which *R* is the gas constant and *T* the absolute temperature.

## Acknowledgements

This work was financially supported by the Spanish Government (CTQ2015-69021-R, CTQ2012-34790, CTQ2014-61470-EXP) and the Xunta de Galicia (GRC2014/040). M.F.-V. thanks the Spanish Government for a FPU Fellowship.

**Keywords:** carbohydrate-lectin interaction, multivalency, glycodendrimer, PEG-dendritic block copolymer, SPR, ITC

[1] a) C. Fasting, C. A. Schalley, M. Weber, O. Seitz, S. Hecht, B. Koksch, J. Dernedde, C. Graf, E.-W. Knapp, R. Haag, *Angew. Chem. Int. Ed.* **2012**, *51*, 10472-10498; b) M. Mammen, S.-K. Choi, G. M. Whitesides, *Angew. Chem. Int. Ed.* **1998**, *37*, 2754-2794.

[2] C.-H. Wong, Wiley-VCH, Weinheim, **2003**, p. 948.

[3] a) N. Jayaraman, *Chem. Soc. Rev.* **2009**, *38*, 3463-3483; b) R. J. Pieters, *Org. Biomol. Chem.* **2009**, *7*, 2013-2025; c) L. L. Kiessling, T. Young, T. D. Gruber, K. H. Mortell, in *Glycoscience* (Eds.: B. Fraser-Reid, K. Tatsuta, J. Thiem), Springer Berlin Heidelberg, **2008**, pp. 2483-2523; d) T. K. Dam, C. F. Brewer, *Biochemistry* **2008**, *47*, 8470-8476; e) A. Mulder, J. Huskens, D. N. Reinhoudt, *Org. Biomol. Chem.* **2004**, *2*, 3409-3424.

[4] a) Y. M. Chabre, R. Roy, *Adv Carbohydr Chem Biochem* **2010**, *63*, 165-393; b) R. Roy, *Curr. Opin. Struct. Biol.* **1996**, *6*, 692-702.

[5] a) E. M. Munoz, J. Correa, R. Riguera, E. Fernandez-Megia, *J. Am. Chem. Soc.* **2013**, *135*, 5966-5969; b) E. M. Munoz, J. Correa, E. Fernandez-Megia, R. Riguera, *J. Am. Chem. Soc.* **2009**, *131*, 17765-17767.

[6] K. Knop, R. Hoogenboom, D. Fischer, U. S. Schubert, *Angew. Chem. Int. Ed.* **2010**, *49*, 6288-6308.

[7] a) A. Sousa-Herves, R. Riguera, E. Fernandez-Megia, *New J. Chem.* **2012**, *36*, 205–210; b) F. Wurm, H. Frey, *Prog. Polym. Sci.* **2011**, *36*, 1-52.

[8] A. Sousa-Herves, R. Novoa-Carballal, R. Riguera, E. Fernandez-Megia, *The AAPS Journal* **2014**, *16*, 948-961.

[9] a) A. Sousa-Herves, C. Sanchez Espinel, A. Fahmi, A. Gonzalez-Fernandez, E. Fernandez-Megia, *Nanoscale* **2015**, *7*, 3933-3940; b) B. Klajnert, T. Wasiak, M. Ionov, M. Fernandez-Villamarin, A. Sousa-Herves, J. Correa, R. Riguera, E. Fernandez-Megia, *Nanomedicine (New York, NY, U. S.)* **2012**, *8*, 1372-1378; c) F. Fernández-Trillo, J. Pacheco-Torres, J. Correa, P. Ballesteros, P. Lopez-Larrubia, S. Cerdán, R. Riguera, E. Fernandez-Megia, *Biomacromolecules* **2011**, *12*, 2902-2907; d) R. Doménech, O. Abian, R. Bocanegra, J. Correa, A. Sousa-Herves, R. Riguera, M. G. Mateu, E. Fernandez-Megia, A. Velázquez-Campoy, J. L. Neira, *Biomacromolecules* **2010**, *11*, 2069-2078; e) A. Sousa-Herves, E. Fernandez-Megia, R. Riguera, *Chem. Commun.* **2008**, 3136-3138.

[10] a) E. Fernandez-Megia, J. Correa, I. Rodríguez-Meizoso, R. Riguera, *Macromolecules* **2006**, *39*, 2113-2120; b) E. Fernandez-Megia, J. Correa, R. Riguera, *Biomacromolecules* **2006**, *7*, 3104-3111.

[11] a) E. Lallana, A. Sousa-Herves, F. Fernandez-Trillo, R. Riguera, E. Fernandez-Megia, *Pharm. Res.* **2012**, *29*, 1-34; b) E. Lallana, F. Fernandez-Trillo, A. Sousa-Herves, R. Riguera, E. Fernandez-Megia, *Pharm. Res.* **2012**, *29*, 902-921; c) M. Meldal, C. W. Tornøe, *Chem. Rev.* **2008**, *108*, 2952-3015; d) V. V. Rostovtsev, L. G. Green, V. V. Fokin, K. B. Sharpless, *Angew. Chem. Int. Ed.* **2002**, *41*, 2596-2599; e) C. W. Tornøe, C. Christensen, M. Meldal, *J. Org. Chem.* **2002**, *67*, 3057-3064.

[12] L. Albertazzi, M. Fernandez-Villamarin, R. Riguera, E. Fernandez-Megia, *Bioconjugate Chem.* **2012**, *23*, 1059-1068.

[13] M. de la Fuente, M. Ravina, A. Sousa-Herves, J. Correa, R. Riguera, E. Fernandez-Megia, A. Sanchez, M. J. Alonso, *Nanomedicine (Lond)* **2012**, *7*, 1667-1681.

[14] a) M. Sawa, T. L. Hsu, T. Itoh, M. Sugiyama, S. R. Hanson, P. K. Vogt, C. H. Wong, *Proc Natl Acad Sci U S A* **2006**, *103*, 12371-12376; b) D. H. Dube, C. R. Bertozzi, *Nat Rev Drug Discov* **2005**, *4*, 477-488; c) D. J. Becker, J. B. Lowe, *Glycobiology* **2003**, *13*, 41R-53R.

[15] M. Raviña, M. de la Fuente, J. Correa, A. Sousa-Herves, J. Pinto, E. Fernandez-Megia, R. Riguera, A. Sanchez, M. J. Alonso, *Macromolecules* **2010**, *43*, 6953-6961.

[16] D. J. Gravert, K. D. Janda, *Chem. Rev.* **1997**, *97*, 489-510.

[17] G. B. Sigal, M. Mammen, G. Dahmann, G. M. Whitesides, *J. Am. Chem. Soc.* **1996**, *118*, 3789-3800.

[18] G. F. Audette, M. Vandonselaar, L. T. J. Delbaere, *J. Mol. Biol.* **2000**, *304*, 423-433.

[19] O. Hindsgaul, D. P. Khare, M. Bach, R. U. Lemieux, *Can. J. Chem.* **1985**, *63*, 2653-2658.

[20] J. B. Corbell, J. J. Lundquist, E. J. Toone, *Tetrahedron: Asymmetry* **2000**, *11*, 95-111.

[21] T. Dam, C. F. Brewer, in *Galectins, Vol. 1207* (Eds.: S. R. Stowell, R. D. Cummings), Springer New York, **2015**, pp. 75-90.

[22] T. K. Dam, C. F. Brewer, *Chem. Rev.* **2002**, *102*, 387-430.

[23] a) H. Lee, R. G. Larson, *Macromolecules* **2011**, *44*, 2291-2298; b) S. Natali, J. Mijovic, *Macromolecules* **2009**, *42*, 6799-6807; c) H. Lee, R. M. Venable, A. D. MacKerell, Jr., R. W. Pastor, *Biophys J.*, *95*, 1590-1599.

[24] G. M. Pavan, A. Barducci, L. Albertazzi, M. Parrinello, *Soft Matter* **2013**, *9*, 2593-2597.

[25] H. Yang, J. J. Morris, S. T. Lopina, *J. Colloid Interface Sci.* **2004**, *273*, 148-154.

[26] L. Albertazzi, F. M. Mickler, G. M. Pavan, F. Salomone, G. Bardi, M. Panniello, E. Amir, T. Kang, K. L. Killops, C. Bräuchle, R. J. Amir, C. J. Hawker, *Biomacromolecules* **2012**, *13*, 4089-4097.

[27] S. P. Amaral, M. Fernandez-Villamarin, J. Correa, R. Riguera, E. Fernandez-Megia, *Org. Lett.* **2011**, *13*, 4522-4525.

[28] B. Johnsson, S. Lofas, G. Lindquist, *Anal Biochem* **1991**, *198*, 268-277.

**Entry for the Table of Contents** (Please choose one layout)

Layout 2:

# FULL PAPER

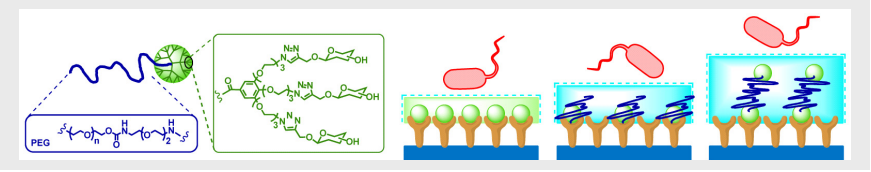


A general synthetic strategy to glycosylated PEG-GATG (gallic acid−triethylene glycol) block copolymers is described as a toolbox to analyze the steric stabilization of PEG (various molecular weights and architectures) on the multivalent binding with lectins by surface plasmon resonance (SPR) and isothermal titration calorimetry (ITC).

*M. Fernandez-Villamarin, A. Sousa-Herves, J. Correa, E. M. Munoz, P. Taboada, R. Riguera, E. Fernandez-Megia**

***Page No. – Page No.***

**The Effect of PEGylation on Multivalent Binding: A SPR and ITC Study with Structurally Diverse PEG-Dendritic GATG Copolymers**

Additional Author information for the electronic version of the article.

A. Sousa-Herves: orcid.org/0000-0003-0111-9057
R. Riguera orcid.org/0000-0001-5133-0454
E. Fernandez-Megia: orcid.org/0000-0002-0405-4933